# Estimation of Hydrodynamic Coefficients for an AUV Using Nonlinear Observers

Joonyoung Kim, Kihun Kim, Hang S. Choi, *Member, IEEE*, Woojae Seong, and Kyu-Yeul Lee

***Abstract*—Hydrodynamic coefficients strongly affect the dynamic performance of an autonomous underwater vehicle. Although these coefficients are generally obtained experimentally such as through the planar-motion-mechanism (PMM) test, the measured values are not completely reliable because of experimental difficulties and errors involved. Another approach by which these coefficients can be obtained is the observer method, in which a model-based estimation algorithm predicts the coefficients. In this paper, the hydrodynamic coefficients are estimated using two nonlinear observers—a sliding mode observer and an extended Kalman filter. Their performances are evaluated by comparing the estimated coefficients obtained from the two observer methods with the values as determined from the PMM test. By using the estimated coefficients, a sliding mode controller is constructed for the diving and steering maneuver. It is demonstrated that the controller with the estimated values maintains the desired depth and path with sufficient accuracy.**

***Index Terms*—Autonomous underwater vehicle (AUV), extended Kalman filter (EKF), hydrodynamic coefficients, nonlinear observer, sliding mode control, sliding mode observer (SMO).**

## I. Introduction

In RECENT years, there have been intensive efforts toward the development of autonomous underwater vehicles (AUVs) (see for example, Wernli [1]). To design an AUV, its maneuverability and controllability must be examined in advance preferably based on a mathematical model. The mathematical model contains hydrodynamic forces and moments expressed in terms of a set of hydrodynamic coefficients. Therefore, it is important to know the true values of these coefficients to simulate the performance of the AUV accurately.

The hydrodynamic coefficients may be classified into three types: linear damping coefficients, linear inertial force coefficients, and nonlinear damping coefficients. Among these, the linear damping coefficients mostly affect the maneuverability of an AUV. Sen [2] examined the influence of various hydrodynamic coefficients on the predicted maneuverability quality of submerged bodies and found that the trajectories are most sensitive to the linear damping coefficients. These coefficients are normally determined by experiments, numerical analysis or empirical formula. Although planar-motion-mechanism (PMM) tests are the most popular among experimental tests, the measured data from these tests are not completely reliable because of experimental difficulties and errors involved.

Another approach that estimates the hydrodynamic coefficients is the observer method, in which a model-based estimation algorithm is used. A representative method among observer methods is the Kalman filter, which has been widely used to estimate state variables and parameters. Hwang [3] estimated the maneuvering coefficients of a ship and identified the dynamic system of a maneuvering ship using an extended Kalman filtering (EKF) technique.

These estimated coefficients are used as input not only for a mathematical model to analyze the AUV's maneuvering performance, but also for a controller to design the AUV's autopilot. Antonelli *et al.* [4] obtained the velocity of the vehicle-manipulator system using an observer, and applied it to tracking control law. Fossen and Blanke [5] designed the speed controller for a propeller shaft by using nonlinear control theory and feedback from the estimated axial flow velocity. Farrell and Clauberg [6] used an EKF as a parameter estimator with pole placement to design successfully the controller of the Sea Squirt vehicle. Yuh [7] described the functional form of the vehicle dynamic equations of motion, the nature of loadings and the use of adaptive control via online parameter identification. McGookin [8] designed the sliding mode controller, which is a reconfiguration process based on a sliding mode observer (SMO), for the heading maneuver of a submarine model.

Recently, advanced control techniques have been developed for AUVs, aiming at improving the capability to track the desired position and attitude. Because of robustness for modeling uncertainty, i.e., variation from operating condition and disturbance, the sliding mode control has been successfully applied to AUV. Cristi *et al.* [9] proposed an adaptive sliding mode controller for AUVs based on the dominant linear model and the bound of nonlinear dynamic perturbations. Healey and Lienard [10] described a 6 degree of freedom (DOF) model for an underwater vehicle and designed a sliding mode autopilot for combined steering, diving, and speed-control functions. Lee *et al.* [11] designed a discrete-time quasi-sliding mode controller for an AUV in the presence of parameter uncertainty and long sampling interval.

In this paper, the hydrodynamic coefficients are estimated based on two nonlinear observers, the SMO and the EKF. The estimated values are compared with the values obtained from the PMM test. These values are applied to design a controller for depth and heading. Because the AUV system to be controlled is highly nonlinear, a sliding mode control is constructed to compensate the effects of modeling nonlinearity, parameter uncertainty, and disturbance.

Manuscript received February 27, 2002; revised September 2, 2002. This work was supported by the Ministry of Science and Technology of Korea, under the Naval Research Laboratory program.

The authors are with the Department of Naval Architecture & Ocean Engineering, Seoul National University, Seoul 151-742, Korea (e-mail: jkimor@gong.snu.ac.kr; kihunkim@orgio.net; hschoi@plaza.snu.ac.kr; kylee@plaza.snu.ac.kr; wseong@snu.ac.kr).

Digital Object Identifier 10.1109/JOE.2002.805098

0364–9059/02$17.00 © 2002 IEEE

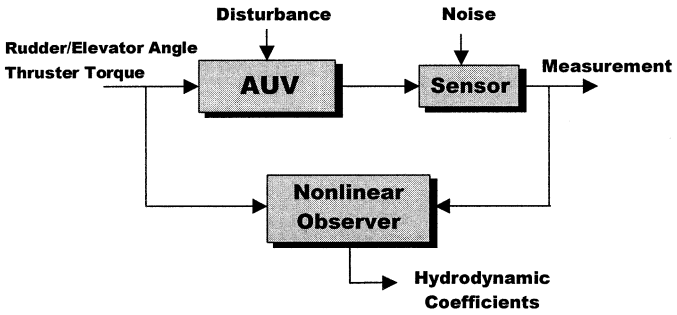



Fig. 1. Configuration of the estimation system.

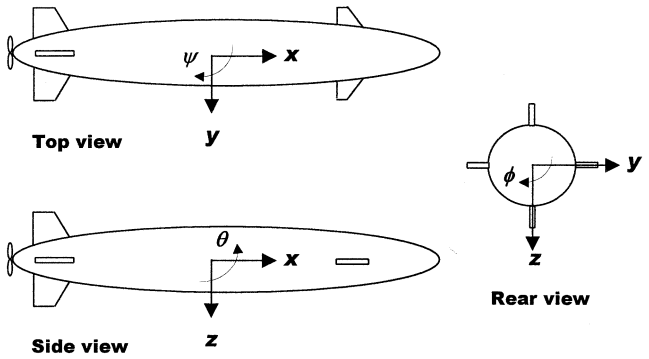



Fig. 2. Coordinate system.

This paper is organized as follows.Section II describes the nonlinear observers for estimating the hydrodynamic coefficients. Section III shows estimation results. Section IV deals with a sliding mode control for depth and heading control. Finally, Section V presents the conclusions.

## II. Estimation of Hydrodynamic Coefficients

The coefficients, which mostly affect the dynamic performance of an AUV, are the linear damping coefficients. Representative linear damping coefficients are composed of 17 elements from five motions as represented in [2], $M_q$, $M_{\delta s}$, $M_w$, $N_r$, $N_{\delta r}$, $N_v$, $N_p$, $Z_{\delta s}$, $Z_q$, $Z_w$, $Y_{\delta r}$, $Y_r$, $Y_v$, $Y_p$, $K_p$, $K_r$, and $K_v$. Among these, $M_q$, $M_{\delta s}$, and $M_w$ are the coefficients associated with pitch motion; $N_r$, $N_{\delta r}$, $N_v$ and $N_p$ are with yaw motion; $Z_{\delta s}$, $Z_q$ and $Z_w$ are with heave motion; $Y_{\delta r}$, $Y_r$, $Y_v$ and $Y_p$ are with sway motion; and $K_p$, $K_r$ and $K_v$ are with roll motion. In this paper, a coefficient estimation system based on nonlinear observers, as illustrated in Fig. 1, is constructed to estimate the 17 linear damping coefficients. The nonlinear observer block is composed of SMO or EKF, which are designed based on the AUV's 6 DOF equations of motion. The measured signals generated from the AUV's motion are used to develop the two nonlinear observers for estimating the linear damping coefficients. The AUV block represents the real plant and includes a 6 DOF nonlinear model of the NPS AUV II [10]. The values of the linear damping coefficients resulting from this block are used as true values and then compared with the estimated ones.

In nonlinear observers, 6 DOF AUV equations of motion and the augmented states for the linear damping coefficients are included. Thus, the observer model describes surge, sway, heave, roll, pitch, and yaw motions. The coordinate system is shown in Fig. 2. The 6 DOF equations of motion for the observer model are as follows:

$$\begin{aligned}
&\text{Surge:} && m[\dot{u} - vr + wq + z_G(pr + \dot{q})] = X \\
&\text{Sway:} && m[\dot{v} + ur - wp + z_G(qr - \dot{p})] = Y \\
&\text{Heave:} && m[\dot{w} - uq + vp - z_G(p^2 + q^2)] = Z \\
&\text{Roll:} && I_x\dot{p} + (I_z - I_y)qr + I_{xy}(pr - \dot{q}) - I_{yz}(q^2 - r^2) \\
& && \quad -I_{xz}(pq + \dot{r}) - mz_G(\dot{v} + ur - wp) = K \\
&\text{Pitch:} && I_y\dot{q} + (I_x - I_z)pr - I_{xy}(qr + \dot{p}) + I_{yz}(pq - \dot{r}) \\
& && \quad +I_{xz}(p^2 - r^2) + mz_G(\dot{u} - vr + wq) = M \\
&\text{Yaw:} && I_z\dot{r} + (I_y - I_x)pq - I_{xy}(p^2 - q^2) - I_{yz}(pr + \dot{q}) \\
& && \quad +I_{xz}(qr - \dot{p}) = N
\end{aligned} \tag{1}$$

where $u$, $v$, and $w$ are the velocity of surge, sway, and heave motion and $p$, $q$, and $r$ are angular velocity of roll, pitch, and yaw motion, respectively. $X$, $Y$, $Z$, $K$, $M$, and $N$ represent the resultant forces and moments with respect to $x$, $y$, and $z$ axis, in this order, and their detailed expressions and nomenclatures are described in [10]. In order to estimate the linear damping coefficients, these coefficients have to be modeled as extra state variables. Consequently, the observer model (1) is transformed into augmented state-space form

$$\begin{bmatrix} \dot{u} \\ \dot{v} \\ \dot{w} \\ \dot{p} \\ \dot{q} \\ \dot{r} \\ \dot{\phi} \\ \dot{\theta} \\ \dot{\psi} \\ \dot{\xi} \end{bmatrix} = [\boldsymbol{M}]^{-1} \begin{bmatrix} X' + X_m \\ Y' + Y_m \\ Z' + Z_m \\ K' + K_m \\ M' + M_m \\ N' + N_m \\ p + q\sin\phi\tan\theta + r\cos\phi\tan\theta \\ q\cos\phi - r\sin\phi \\ (q\sin\phi + r\cos\phi)\sec\theta \\ 0 \end{bmatrix} \tag{2}$$

where $\phi$, $\theta$, and $\psi$ are the angle of roll, pitch, and yaw, respectively. $\boldsymbol{M}$ is the inertia matrix and the extra state $\xi$ denotes the linear damping coefficients. $X'$, $Y'$, $Z'$, $K'$, $M'$, and $N'$ represent the external forces and moments except acceleration components. $X_m$, $Y_m$, $Z_m$, $K_m$, $M_m$, and $N_m$ stand for the components of the inertial forces and moments. The detailed expressions are shown in the Appendix. Therefore, nonlinear observers are designed based on (2).

### A. SMO

The SMO, which is developed on the basis of the sliding surface concept [12], can set the gain value according to the uncertainty range of the plant model. The SMO is known to be robust to parameter uncertainty and disturbance. Besides, it can be easily applied to the nonlinear system [13]. In general, a nonlinear system may be represented by

$$\begin{aligned} \dot{x} &= f(x, t) \\ y &= Cx \end{aligned} \tag{3}$$

where $x \in R^n$ is the state vector, $y \in R^m$ is the measurement vector, $f(x, t)$ is the true plant and $C \in R^{m \times n}$ is the measure-

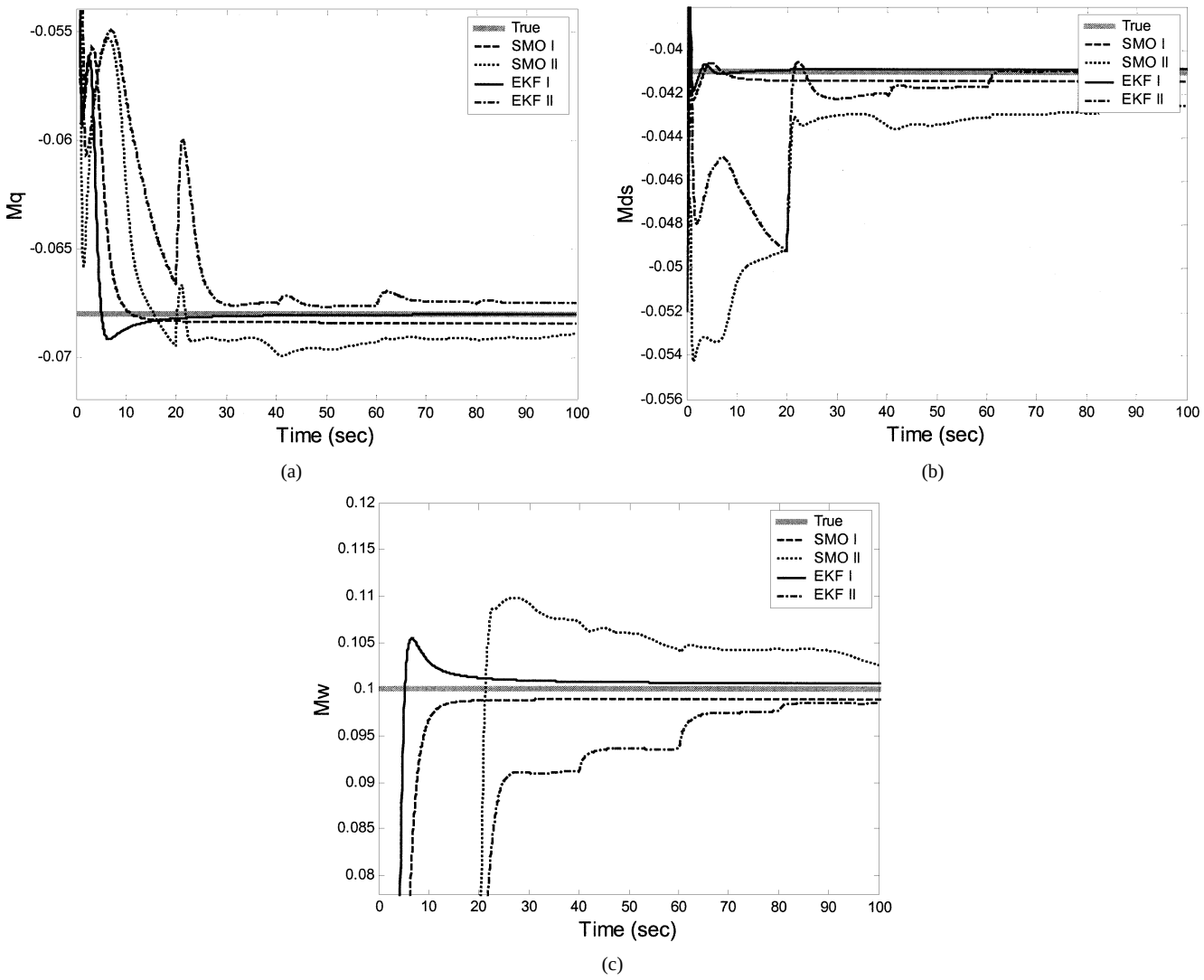



Fig. 3. Estimation results of pitch coefficients. (a) $M_q$. (b) $M_{\delta s}$. (c) $M_w$.

ment matrix. The measurement is assumed to be a linear combination of the state, and the inputs are contained in $f(x, t)$. If we define a sliding surface $s$ as the error $\tilde{y}$

$$s = \tilde{y} = \hat{y} - y = C(\hat{x} - x) \tag{4}$$

then, the sliding surface converges to zero when it satisfies the Lyapunov stability as follows:

$$s\dot{s} = \tilde{y}\dot{\tilde{y}} < 0. \tag{5}$$

Inequality (5) is referred to as the sliding condition. If (5) is satisfied, the sliding surface $s = 0$ is guaranteed and the error $\tilde{y}$ tends toward zero. In order to satisfy the sliding condition, the SMO is given by

$$\dot{\hat{x}} = f(\hat{x}, t) - L\tanh(\tilde{y}/\Phi) \tag{6}$$

where $L$ is the nonlinear gain matrix to be determined and $\tanh(\tilde{y}/\Phi)$ represents the switching term which uses the "tanh" function instead of "sign" function. $\Phi$ is the boundary layer thickness and it acts as a low-pass filter to remove chattering and noise. From (3) and (6), the error dynamics is given by

$$\begin{aligned}\dot{\tilde{x}} &= \dot{\hat{x}} - \dot{x} \\ &= f(\hat{x}, t) - f(x, t) - L\tanh(\tilde{y}/\Phi) \\ &= \Delta f(\tilde{x}, t) - L\tanh(\tilde{y}/\Phi)\end{aligned} \tag{7}$$

where $f(\hat{x}, t)$ is the modeled plant. The value of $\Delta f(\tilde{x}, t)$ depends both on the modeling complexity and on the error magnitude. Using the error dynamics (7), the sliding condition is as follows:

$$\tilde{y}\dot{\tilde{y}} = \tilde{y}C\dot{\tilde{x}} = \tilde{y}C(\Delta f - L\tanh(\tilde{y}/\Phi)) < 0. \tag{8}$$

To satisfy (8), given bounds on $\Delta f$, the nonlinear gain $L$ is chosen by

$$L_i > |\Delta f_i(\tilde{x}, t)|, \qquad i = 1 \sim p. \tag{9}$$

Here, $L_i$ is the $p$th-order nonlinear gain. In addition, during sliding, namely when the sliding surface goes to zero, the switching term can be written from (8)

$$\tanh(\tilde{y}/\Phi) \approx (CL)^{-1}C\Delta f. \tag{10}$$

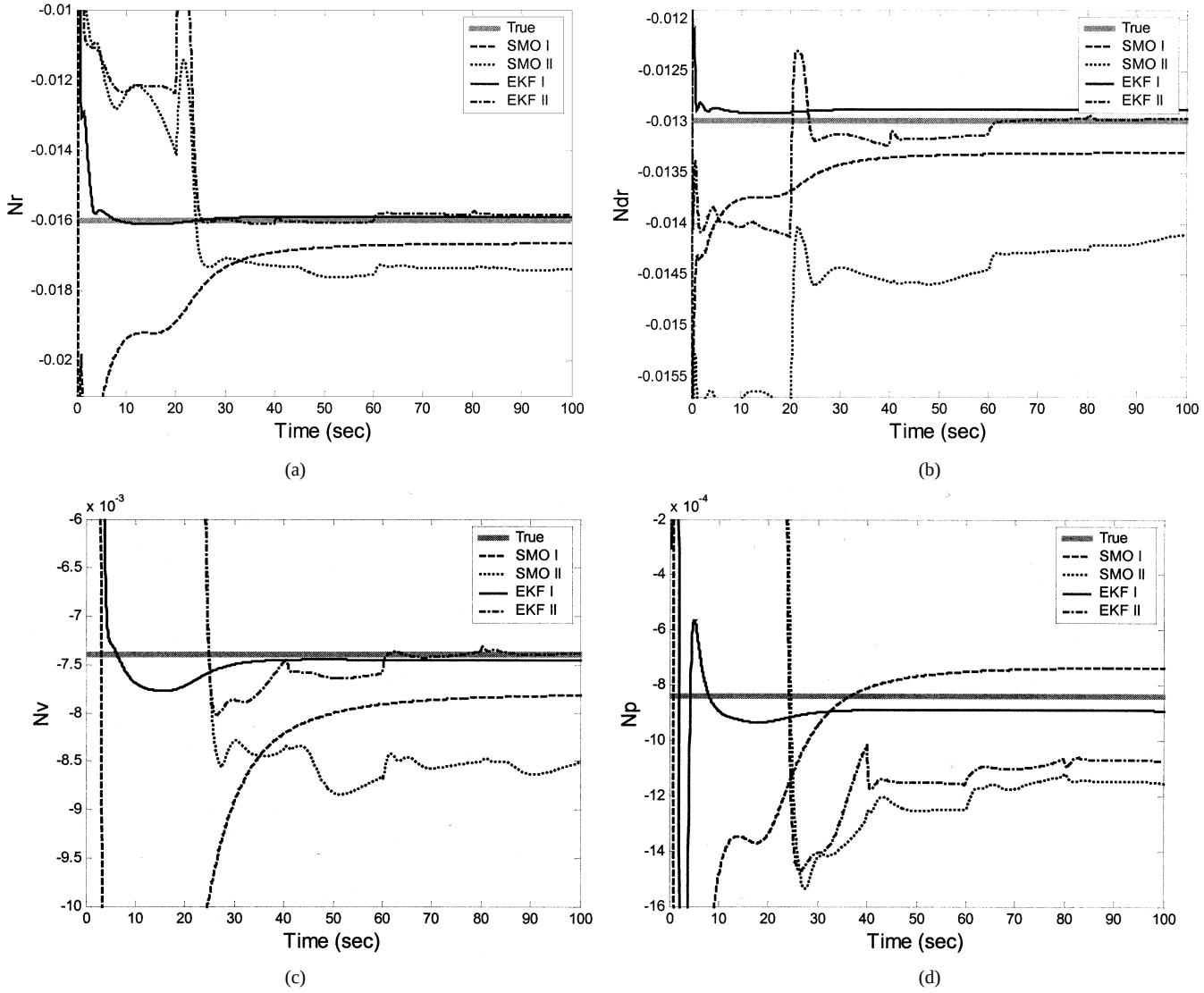



Fig. 4. Estimation results of yaw coefficients. (a) $N_r$. (b) $N_{\delta r}$. (c) $N_v$. (d) $N_p$.

From (10), the error dynamics (7) is developed by

$$\dot{\tilde{x}} \approx [I - L(CL)^{-1}C]\Delta f \tag{11}$$

where $I$ implies the identity matrix. Therefore, the system dynamics are reduced from the $n$th order to the $n-p$th order during sliding. The equation has the form of $\dot{\tilde{x}} = \alpha\tilde{x}$, so, the nonlinear gain matrix $L$ is chosen such that $\alpha$ has a negative eigenvalue.

In order to estimate the hydrodynamic coefficients, the SMO is designed using the observer model (2). The state variable yields to $x = [u\ v\ w\ p\ q\ r\ \phi\ \theta\ \psi\ M_q\ M_{\delta s}\ M_w\ N_r\ N_{\delta r}\ N_v\ N_p\ Z_{\delta s}\ Z_q\ Z_w\ Y_{\delta r}\ Y_r\ Y_v\ Y_p\ K_p\ K_r\ K_v]^T$. The output variables are chosen as two types according to the measurement. The first output uses velocity measurements such as $y = [u\ v\ w\ p\ q\ r\ \phi\ \theta\ \psi]^T$ and then, the second output uses acceleration measurements such as $y = [a_x\ a_y\ a_z\ p\ q\ r\ \phi\ \theta\ \psi]^T$ that can be applied to a real plant.

### *B. EKF*

The EKF can estimate the state variables optimally in nonlinear stochastic cases that include plant perturbation and sensor noise. In particular, unknown input or parameters can be estimated by converting them to extra state variables [14]. Assume that a system, which contains unknown parameters, is given as

$$\begin{aligned} x_{k+1} &= f(x_k, \xi_k, k) + w_k \\ y_k &= h(x_k, \xi_k, k) + v_k \end{aligned} \tag{12}$$

where $x \in R^n$ is the state vector, $y \in R^m$ is the measurement vector, $\xi \in R^p$ is the unknown parameter vector, and $v$ is the sensor noise. In order to estimate the unknown parameters, the state variable $x$ is augmented by the unknown parameters. Therefore, (12) can be expressed in augmented state-space form as

$$\begin{aligned} x^*_{k+1} &= \begin{bmatrix} x_{k+1} \\ \xi_{k+1} \end{bmatrix} = \begin{bmatrix} f(x_k, \xi_k, k) \\ 0 \end{bmatrix} + \begin{bmatrix} w_k \\ \eta_k \end{bmatrix} \\ y_k &= h(x^*_k, k) + v_k \end{aligned} \tag{13}$$

where $w \in R^n$, $\eta \in R^p$ and $\nu \in R^m$ are zero-mean Gaussian white noise sequences and $x^* \in R^{n+p}$ is the augmented state vector. For this system, the discrete-time EKF is ummarized

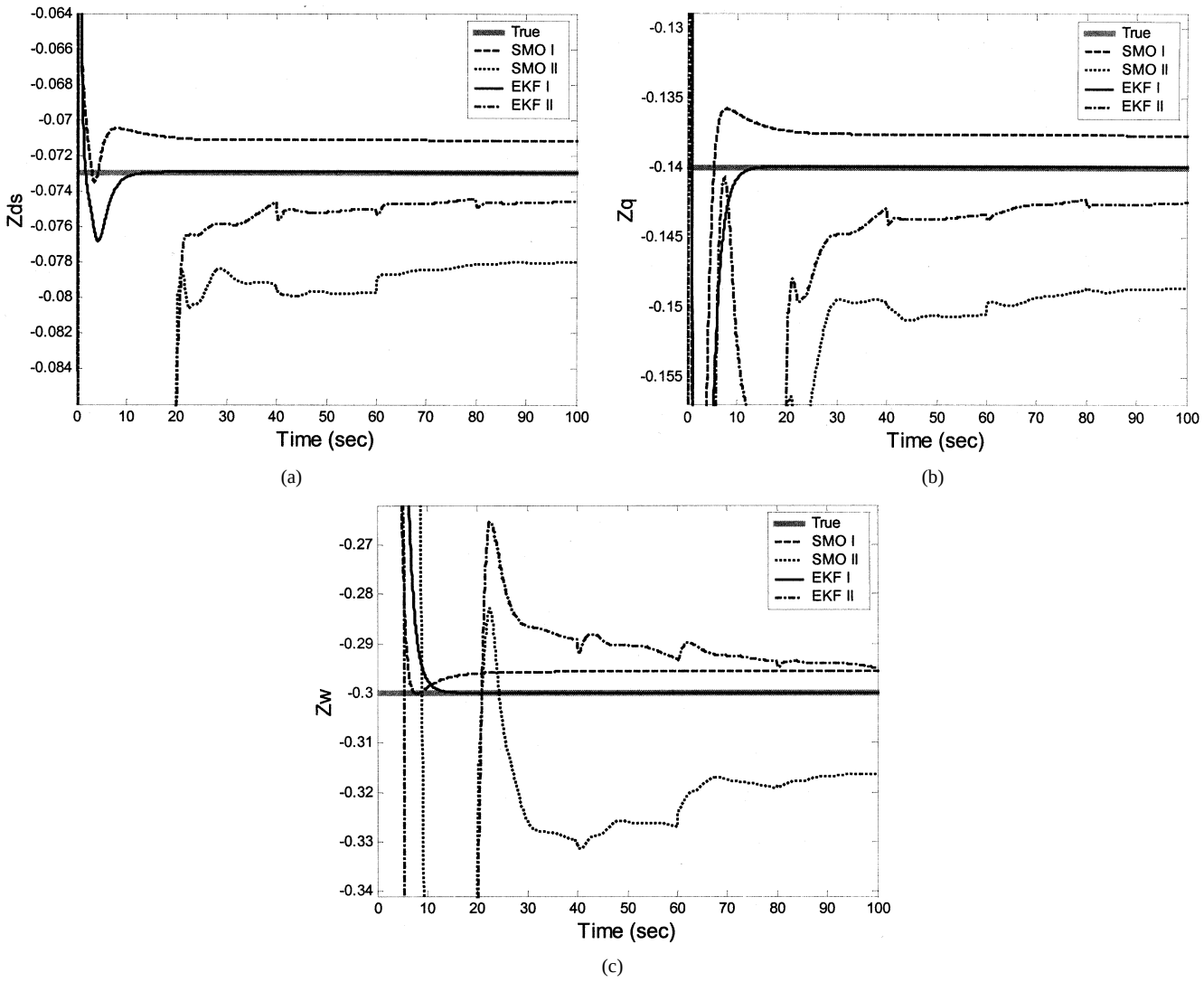



Fig. 5. Estimation results of heave coefficients. (a) $Z_{\delta s}$. (b) $Z_q$. (c) $Z_w$.

as

Time update:

$$\hat{x}^*_{k+1}(-) = f(\hat{x}^*_k(+),\, k) \tag{14}$$

$$P_{k+1}(-) = F^*_k P_k(+) F^{*T}_k + Q_k \tag{15}$$

Measurement update:

$$K_k = P_k(-) H^{*T}_k [H^*_k P_k(-) H^{*T}_k + R_k]^{-1} \tag{16}$$

$$\hat{x}^*_k(+) = \hat{x}^*_k(-) + K_k[y_k - h(\hat{x}^*_k(-),\, k)] \tag{17}$$

$$P_k(+) = [I - K_k H^*_k]^P_k(-) \tag{18}$$

where

$$F^*_k = \left.\frac{\partial f(x^*,\, k)}{\partial x^*}\right|_{x^* = \hat{x}^*_k(+)} \qquad H^*_k = \left.\frac{\partial h(x^*,\, k)}{\partial x^*}\right|_{x^* = \hat{x}^*_k(-)}$$

$P$ is the error covariance and $Q$ is the process noise covariance. The gain matrix $K$ is determined from the Riccati equation and the measurement noise covariance $R$ is determined by satisfying the Lyapunov function of error [15]. Time updates (14) and (15) mean extrapolation by state transition matrix and measurement updates (16)–(18) reflect the actual measurement process by optimal gain $K$.

To estimate the hydrodynamic coefficients, the EKF is designed using the observer model of (2). The 17 linear damping coefficients, which are represented by $\xi$, are estimated through (14)–(18). The state and output variables are equal to those of the SMO.

## III. Estimation Results

The linear damping coefficients associated with horizontal and vertical motions are estimated by simulating the combined diving and steering motion of the AUV. The linear damping coefficients adopted from [10] are used as true values and compared with the estimated ones. The SMO and the EKF are designed in two types according to the measurement. First, SMO I and EFK I use velocity measurements such as $y = [u\ v\ w\ p\ q\ r\ \phi\ \theta\ \psi]^T$ and then, SMO II and EKF II use acceleration measurements such as $y = [a_x\ a_y\ a_z\ p\ q\ r\ \phi\ \theta\ \psi]^T$. In fact, velocity is more difficult to measure than acceleration. While the SMO I and the EKF I can only estimate the coefficients in simulation, the SMO II and the EKF II can be

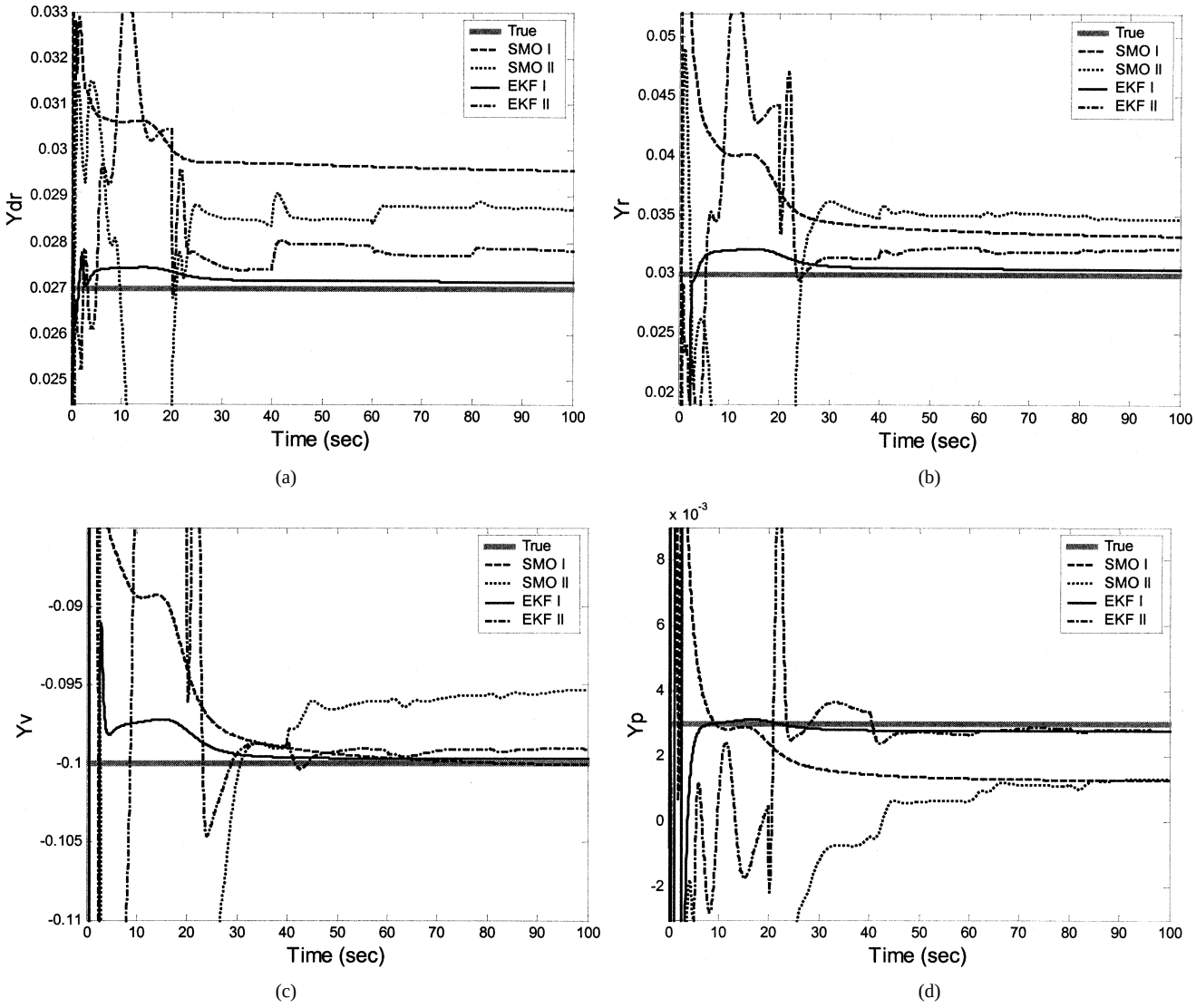



Fig. 6. Estimation results of sway coefficients. (a) $Y_{\delta r}$. (b) $Y_r$. (c) $Y_v$. (d) $Y_p$.

implemented to a real AUV system using an accelerometer and gyroscope. The estimation is reviewed for accuracy when the AUV undergoes combined diving and steering. Two types of motion scenarios are presented as follows.

1) For the SMO I and the EKF I, the AUV has a spiral motion. It has an initial speed of 1.8 m/s and the rudder/elevator angle applies to 0.35 rad from the start.
2) For the SMO II and the EKF II, the AUV undergoes a zigzag motion. It has the same initial speed as in 1) and the rudder/elevator angle changes from 0.35 to $-0.35$ rad at 20 s. The rudder and elevator works within $-0.4$ to 0.4 rad.

Figs. 3–7 compare the estimation results of the SMO I, SMO II, EKF I, and EKF II for the 17 linear damping coefficients. The steady-state errors of the coefficients are compared in Table I. The noise-free data are measured to distinguish the estimation performance of the four observers exactly. In the figures, the thick solid line represents the true value and the dashed/dotted/solid/dashdot lines correspond to the SMO I/SMO II/EKF I/EKF II results, respectively. The SMO I estimates the coefficients with sufficient accuracy, although $N_p$, $Y_{\delta r}$, $Y_r$, and $Y_p$ contain large steady-state errors. The SMO II shows poor estimation performance as a whole. The EKF I predicts the coefficients exactly but $N_p$, $Y_r$, and $Y_p$ contain some steady-state errors, while the EKF II render those with sufficient accuracy, although the magnitude of the error for $N_p$, $Y_r$, and $Y_p$ was larger. In general, the EKF estimates better than the SMO. More precisely, the EKF I predicts the values more exactly, as demonstrated in terms of the average values of estimation error given in Table I. It is well known that the SMO is robust under parameter uncertainty and disturbance, but the SMO II has large steady-state error and fluctuation in the transient period. A series of simulations seems to indicate that the EKF predicts the linear damping coefficients with sufficient accuracy. Although nonlinear observers have been traditionally used in simulation, the EKF II can be implemented instead of the PMM test.

The trajectories are plotted to cast the accuracy of the estimated coefficients. Fig. 8 shows the trajectories resulting from the EKF I values with those of the EKF II values when the AUV undergoes a spiral motion. Fig. 8(a) represents the three-dimensional trajectory and Fig. 8(b) shows its projection on the ver-

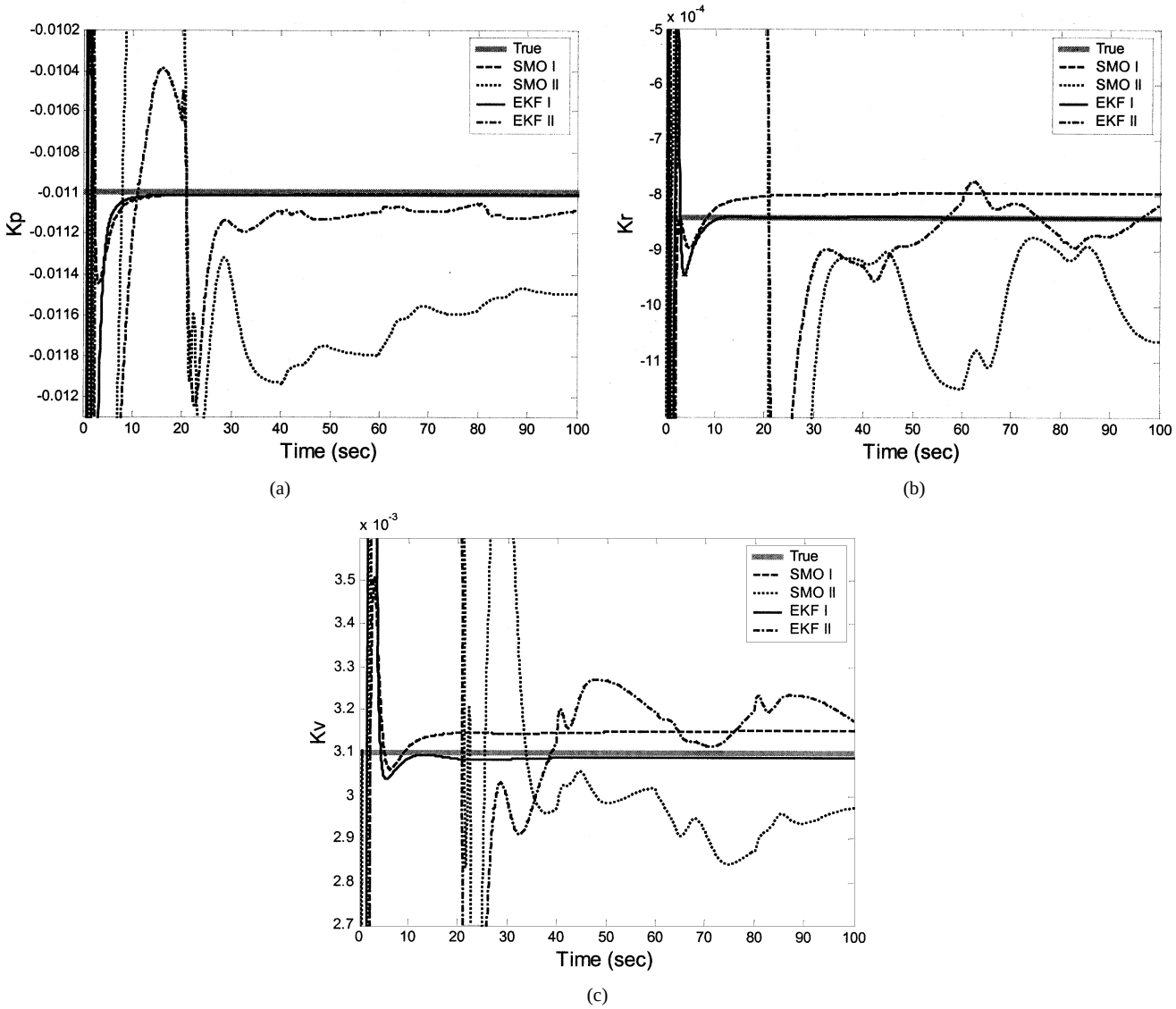



Fig. 7. Estimation results of roll coefficients. (a) $K_p$. (b) $K_r$. (c) $K_v$.

tical plane. In the figures, the trajectory with the EKF I values is exactly the same as the true one and the trajectory with the EKF II values has the same trend but with a continuous deviation of about 10 cm. This implies that all the linear damping coefficients of the EKF II are rightly estimated within an allowable range.

## IV. Application for Control

Although an AUV is difficult to control because of high nonlinearity and coupled motion, sliding mode controls have been successfully applied to underwater vehicles [8]–[11]. In this paper, a sliding mode control is adopted for an AUV with system parameter uncertainties. Especially, when designing a sliding mode controller, the estimated hydrodynamic coefficients explained in Section III are used in the controller model.

It is well known that the sliding mode control provides effective and robust ways of controlling an uncertain plant by means of a switching control law, which drives the plant's state trajectory onto the sliding surface in the state space. The details of the method can be found in [10].

### A. Depth Control

To design a controller in the vertical plane, the linearized diving system dynamics are developed as follows:

$$\begin{aligned}\left(I_y-\frac{\rho}{2}L^5M_{\dot{q}}\right)\dot{q}&=\left(\frac{\rho}{2}L^4u\hat{M}_q\right)q-(z_G-z_B)W\theta\\&\quad+\left(\frac{\rho}{2}L^3u^2\hat{M}_{\delta s}\right)\delta_s\\\dot{\theta}&=q\\\dot{Z}&=-u\theta.\end{aligned}\tag{19}$$

In (19), the values of $\hat{M}_q$ and $\hat{M}_{\delta s}$ estimated as described in Section III are used. When the EKF II values are used, the dynamic model for depth control yields the state equation given by

$$\begin{bmatrix}\dot{q}\\\dot{\theta}\\\dot{Z}\end{bmatrix}=\begin{bmatrix}-0.9929&-0.0662&0\\1&0&0\\0&-1.8320&0\end{bmatrix}\begin{bmatrix}q\\\theta\\Z\end{bmatrix}+\begin{bmatrix}-0.2074\\0\\0\end{bmatrix}\delta_s.\tag{20}$$

TABLE I
STEADY-STATE ERROR (%)

| | SMO I | SMO II | EKF I | EKF II |
|---|---|---|---|---|
| $M_q$ | 0.63 | 1.36 | 0.05 | 0.74 |
| $M_{\delta s}$ | 0.98 | 3.60 | 0.39 | 0.39 |
| $M_w$ | 1.04 | 2.61 | 0.65 | 1.46 |
| $N_r$ | 4.07 | 8.55 | 0.57 | 1.01 |
| $N_{\delta r}$ | 2.36 | 8.52 | 0.89 | 0.23 |
| $N_v$ | 5.66 | 15.04 | 0.82 | 0.24 |
| $N_p$ | 12.31 | 37.51 | 6.17 | 27.74 |
| $Z_{\delta s}$ | 2.52 | 6.81 | 0.07 | 2.17 |
| $Z_q$ | 1.65 | 6.12 | 0.05 | 1.78 |
| $Z_w$ | 1.46 | 5.50 | 0.03 | 1.65 |
| $Y_{\delta r}$ | 9.48 | 6.33 | 0.58 | 3.04 |
| $Y_r$ | 10.88 | 15.72 | 1.55 | 7.07 |
| $Y_v$ | 0.12 | 4.61 | 0.25 | 0.88 |
| $Y_p$ | 58.12 | 56.61 | 7.60 | 7.20 |
| $K_p$ | 0.09 | 4.54 | 0.14 | 0.78 |
| $K_r$ | 5.28 | 26.76 | 0.01 | 2.61 |
| $K_v$ | 1.64 | 4.14 | 0.38 | 2.45 |
| Average | 6.95 | 12.60 | 1.18 | 3.61 |

The sliding surface is defined when the poles are placed at $[0\ -0.25\ -0.26]$ and

$$s_s = 28.18\tilde{q} + 14.37\tilde{\theta} - \tilde{Z}. \tag{21}$$

Finally, the depth control law is determined as

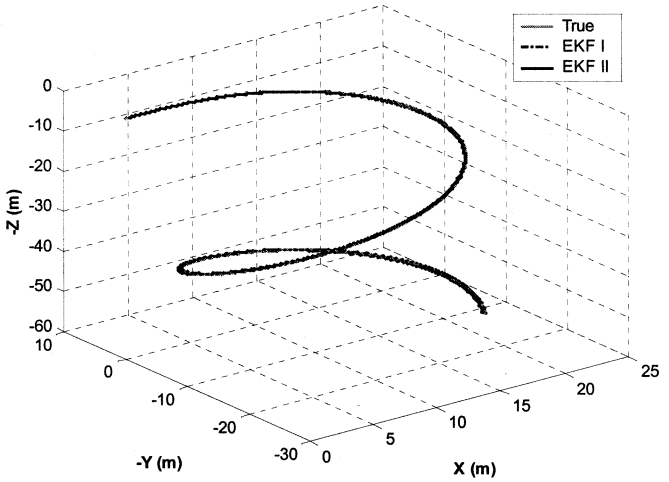
$$\delta_s = 2.3531q + 0.0062\theta - 0.1698\dot{Z}_{\text{com}} + 2.3\tanh(s_s/4). \tag{22}$$

To implement the above depth control law, an AUV has to be equipped with devices measuring for the pitch rate, pitch angle, and depth.

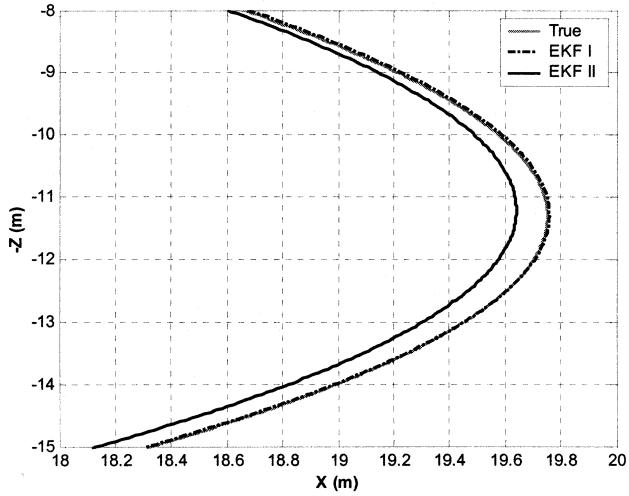
### *B. Heading Control*

The linearized steering system dynamics are given as follows:

$$\begin{aligned}&\left(m - \frac{\rho}{2}L^3Y_{\dot{v}}\right)\dot{v} - \left(\frac{\rho}{2}L^4Y_{\dot{r}}\right)\dot{r}\\ &\quad = \left(\frac{\rho}{2}L^2u\hat{Y}_v\right)v + \left(\frac{\rho}{2}L^3u\hat{Y}_r - mu\right)r + \left(\frac{\rho}{2}L^2u^2\hat{Y}_{\delta r}\right)\delta_r\\ &-\left(\frac{\rho}{2}L^4N_{\dot{v}}\right)\dot{v} + \left(I_z - \frac{\rho}{2}L^5N_{\dot{r}}\right)\dot{r}\\ &\quad = \left(\frac{\rho}{2}L^3u\hat{N}_v\right)v + \left(\frac{\rho}{2}L^4u\hat{N}_r\right)r + \left(\frac{\rho}{2}L^3u^2\hat{N}_{\delta r}\right)\delta_r\\ &\dot{\psi} = r.\end{aligned} \tag{23}$$




(a)




(b)

Fig. 8. Comparison of trajectories. (a) 3-D plot. (b) Projection on *x*–*z* plane.

In (23), the estimated values of $\hat{Y}_v$, $\hat{Y}_r$, $\hat{Y}_{\delta r}$, $\hat{N}_v$, $\hat{N}_r$, and $\hat{N}_{\delta r}$ are used. If the EKF II values are used, the dynamic model for the heading control yields the state equation by

$$\begin{bmatrix}\dot{v}\\ \dot{r}\\ \dot{\psi}\end{bmatrix} = \begin{bmatrix}-0.2697 & -0.6161 & 0\\ -0.0549 & -0.5658 & 0\\ 0 & 1 & 0\end{bmatrix}\begin{bmatrix}v\\ r\\ \psi\end{bmatrix} + \begin{bmatrix}0.1296\\ -0.1539\\ 0\end{bmatrix}\delta_r. \tag{24}$$

When the poles are placed at $[0\ -0.41\ -0.42]$, the sliding surface is defined by

$$s_r = 0.15\tilde{v} + 1.65\tilde{r} + \tilde{\psi}. \tag{25}$$

Finally, the heading control law is defined as follows:

$$\delta_r = 0.5260v + 0.1621r + 4.3465\dot{\psi}_{\text{com}} + 1.5\tanh(s_r/0.05). \tag{26}$$

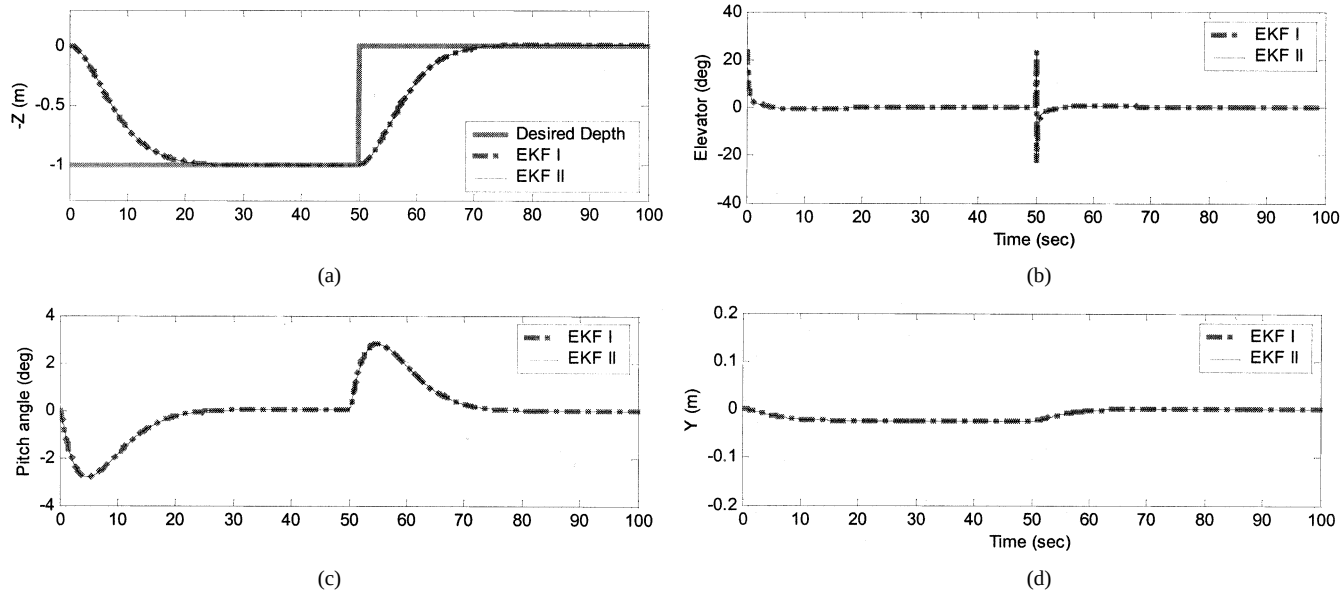



Fig. 9. Simulation results of depth control. (a) Vertical trajectory. (b) Elevator angle. (c) Pitch angle. (d) Horizontal derivation.

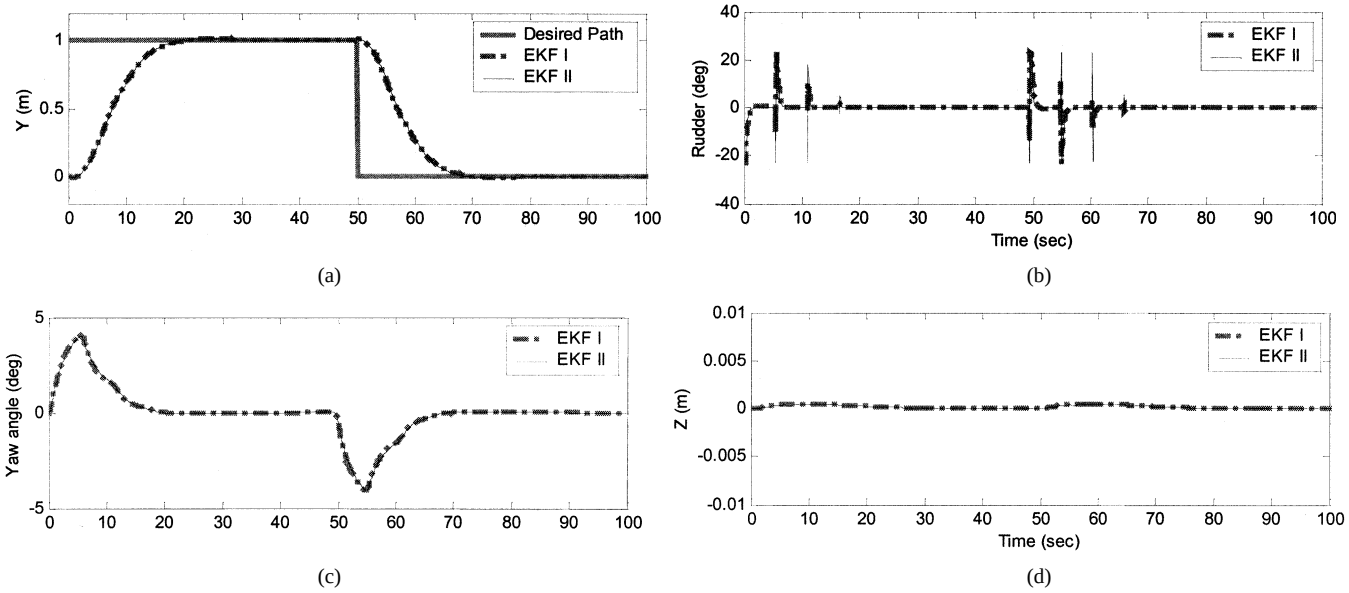



Fig. 10. Simulation results of heading control. (a) Horizontal trajectory. (b) Rudder angle. (c) Yaw angle. (d) Vertical derivation.

To implement the above heading control law, the sway velocity, yaw rate, and yaw angle signals must be measured.

### *C. Simulation Results*

Numerical simulations are made to show the controllability of the AUV under consideration. The simulation program is developed using MATLAB 6.0 under SIMULINK 4.0 environment. The controller block is composed of a sliding mode controller for the depth and heading control. The AUV data of input and output as the true plant are taken from the NPS AUV II [9]. The depth and heading controls are simulated with the full nonlinear equation and the sliding mode controller is developed as given in (22) and (26). The responses of control law with the EKF I values, which are exactly same as the true ones, are compared with those of control law with the EKF II values which contain steady-state errors.

Fig. 9 shows the desired depth, tracking trajectory, and other controlled variables for the depth control simulation, which is carried out with the heading control to avoid the horizontal motion due to coupling. The desired depth is 1 m down from the initial depth during the first 50 s, and then it resumes to the initial depth thereafter. From the figures, it is found that the performance of the EKF II controller is similar to that of the EKF I controller. The EKF II controller, especially, has a good tracking performance despite of the coefficients' deviations, but it shows a slight drift in the sway direction, as can be seen from Fig. 9(d). This result means that the sliding mode control is robust even under parameter uncertainty.

Fig. 10 shows the responses of the heading control, which is control is simulated with depth control to prevent the vertical motion due to coupling. To follow the desired path, we define the line of sight [10] in terms of a desired yaw angle first, and then the proposed heading control follows the desired

yaw angle. The desired path is chosen as 1 m toward the $y$-direction during the first 50 s, and then it takes the initial position. In the figures, the EKF II controller follows the desired path similar to that of the EKF I controller, but the EKF II controller needs a larger rudder angle, as seen in Fig. 10(b). It is to note that the EKF II controller follows the desired path even when the estimated coefficients contain some steady-state errors.

## V. Conclusions

For analyzing the maneuverability and controllability of an AUV, the hydrodynamic coefficients are estimated based on nonlinear observers such as the SMO and the EKF. Simulations clearly demonstrate that the nonlinear observers can estimate the coefficients rightly. More precisely, the EKF shows better estimation performance than the SMO. The EKF with the

$$
\begin{aligned}
X' &= \frac{\rho}{2}L^4[X_{pp}p^2 + X_{qq}q^2 + X_{rr}r^2 + X_{pr}pr] + \frac{\rho}{2}L^3[X_{wq}wq + X_{vp}vp + X_{vr}vr + X_{q\delta s}uq\delta_s + X_{r\delta r}ur\delta_r] \\
&\quad + \frac{\rho}{2}L^2[X_{vv}v^2 + X_{ww}w^2 + X_{v\delta r}uv\delta_r + X_{w\delta s}uw\delta_s + u^2(X_{\delta s\delta s}\delta_s^2 + X_{\delta r\delta r}\delta_r^2)] \\
&\quad - (W-B)\sin\theta + \frac{\rho}{2}L^3X_{q\delta sn}uq\delta_s\varepsilon(n) + \frac{\rho}{2}L^2[X_{\delta s\delta sn}u^2\delta_s^2]\varepsilon(n) + \frac{\rho}{2}L^2u^2X_{\text{prop}} \\
Y' &= \frac{\rho}{2}L^4[Y_{pq}pq + Y_{qr}qr] + \frac{\rho}{2}L^3[Y_pup + Y_rur + Y_{vq}vq + Y_{wp}wp + Y_{wr}wr] \\
&\quad + \frac{\rho}{2}L^2[Y_vuv + Y_{vw}vw + Y_{\delta r}u^2\delta_r] + (W-B)\cos\theta\sin\phi \\
Z' &= \frac{\rho}{2}L^4[Z_{pp}p^2 + Z_{pr}pr + Z_{rr}r^2] + \frac{\rho}{2}L^3[Z_quq + Z_{vp}vp + Z_{vr}vr] + \frac{\rho}{2}L^2[Z_wuw + Z_{vv}v^2 + Z_{\delta s}u^2\delta_s] \\
&\quad + (W-B)\cos\theta\cos\phi + \frac{\rho}{2}L^3Z_{qn}uq\varepsilon(n) + \frac{\rho}{2}L^2[Z_{wn}uw + Z_{\delta sn}u^2\delta_s]\varepsilon(n) \\
K' &= \frac{\rho}{2}L^5[K_{pq}pq + K_{qr}qr] + \frac{\rho}{2}L^4[K_pup + K_rur + K_{vq}vq + K_{wp}wp + K_{wr}wr] + \frac{\rho}{2}L^3[K_vuv + K_{vw}vw] \\
&\quad + (y_GW - y_BB)\cos\theta\cos\phi - (z_GW - z_BB)\cos\theta\sin\phi + \frac{\rho}{2}L^4K_{pn}up\varepsilon(n) + \frac{\rho}{2}L^3u^3K_{\text{prop}} \\
M' &= \frac{\rho}{2}L^5[M_{pp}p^2 + M_{pr}pr + M_{rr}r^2] + \frac{\rho}{2}L^4[M_quq + M_{vp}vp + M_{vr}vr] + \frac{\rho}{2}L^3[M_wuw + M_{vv}v^2 + M_{\delta s}u^2\delta_s] \\
&\quad - (x_GW - x_BB)\cos\theta\cos\phi - (z_GW - z_BB)\sin\theta + \frac{\rho}{2}L^4M_{qn}uq\varepsilon(n) + \frac{\rho}{2}L^3[M_{wn}uw + M_{\delta sn}u^2\delta_s]\varepsilon(n) \\
N' &= \frac{\rho}{2}L^5[N_{pq}pq + N_{qr}qr] + \frac{\rho}{2}L^4[N_pup + N_rur + N_{vq}vq + N_{wp}wp + N_{wr}wr] + \frac{\rho}{2}L^3[N_vuv + N_{vw}vw + N_{\delta r}u^2\delta_r] \\
&\quad + (x_GW - x_BB)\cos\theta\sin\phi + (y_GW - y_BB)\sin\theta + \frac{\rho}{2}L^3u^2N_{\text{prop}} \\
X_m &= m[vr - wq - z_Gpr] \\
Y_m &= -m[ur - wp + z_Gqr] \\
Z_m &= m[uq - vp + z_G(p^2 + q^2)] \\
K_m &= -(I_z - I_y)qr - I_{xy}pr + I_{yz}(q^2 - r^2) + I_{xz}pq + m[z_G(ur - wp)] \\
M_m &= -(I_x - I_z)pr + I_{xy}qr - I_{yz}pq - I_{xz}(p^2 - r^2) - m[z_G(wq - vr)] \\
N_m &= -(I_y - I_x)pq + I_{xy}(p^2 - q^2) + I_{yz}pr - I_{xz}qr
\end{aligned}
$$

$$
M = \begin{bmatrix}
m - \frac{\rho}{2}L^3X_{\dot u} & 0 & 0 & 0 & mz_G & 0 & \vdots & \\
0 & m - \frac{\rho}{2}L^3Y_{\dot v} & 0 & -mz_G - \frac{\rho}{2}L^4Y_{\dot p} & 0 & -\frac{\rho}{2}L^4Y_{\dot r} & \vdots & \\
0 & 0 & m - \frac{\rho}{2}L^3Z_{\dot w} & 0 & -\frac{\rho}{2}L^4Z_{\dot q} & 0 & \vdots & \\
0 & -mz_G - \frac{\rho}{2}L^4K_{\dot v} & 0 & I_x - \frac{\rho}{2}L^5K_{\dot p} & -I_{xy} & -I_{xz} - \frac{\rho}{2}L^5K_{\dot r} & \vdots & 0_{6\times 20} \\
mz_G & 0 & -\frac{\rho}{2}L^4M_{\dot w} & -I_{xy} & I_y - \frac{\rho}{2}L^5M_{\dot q} & -I_{yz} & \vdots & \\
0 & -\frac{\rho}{2}L^4N_{\dot v} & 0 & -I_{xz} - \frac{\rho}{2}L^5N_{\dot p} & -I_{yz} & I_z - \frac{\rho}{2}L^5N_{\dot r} & \vdots & \\
\cdots & \cdots & \cdots & \cdots & \cdots & \cdots & \cdots & \cdots \\
 & & & 0_{20\times 6} & & & \vdots & I_{20\times 20}
\end{bmatrix}
$$

velocity measurements (EKF I) yields the best prediction, while the EKF with the acceleration measurements (EKF II) estimates the coefficients with sufficient accuracy, although it contains some steady-state errors. Thus, it may be concluded that the EKF II method can be implemented on a real AUV by replacing the PMM test for measuring the coefficients. Using the estimated coefficients, a sliding mode controller is designed for the diving and steering maneuvers. Simulations show that the control system with the estimated coefficients guides the vehicle to follow the desired depth and path similar to the system with the true values. It means that the sliding mode control is robust to parameter uncertainties. Thus, the control system with the estimated coefficients makes the AUV stable and controllable.

## APPENDIX

Details of expressions used in Section II are shown at the bottom of the previous page.

## ACKNOWLEDGMENT

This work has been done within the framework of the NRL program. The authors would like to thank the Ministry of Science & Technology, Korea, for the financial support.

## REFERENCES

[1] R. L. Wernli, "AUVs—A technology whose time has come," in *Proc. Conf. UT'02 OES/IEEE* , 2002, pp. 309–314.
[2] D. Sen, "A study on sensitivity of maneuverability performance on the hydrodynamic coefficients for submerged bodies," *J. Ship Res.*, vol. 44, no. 3, pp. 186–196, 2000.
[3] W. Y. Hwang, "Application of system identification to ship maneuvering," Ph.D. dissertation, Massachusetts Inst. Technol., Cambridge, 1980.
[4] G. Antonelli, F. Caccavale, S. Chiaverini, and L. Villani, "Tracking control for underwater vehicle-manipulator systems with velocity estimation," *IEEE J. Oceanic Eng.*, vol. 25, pp. 399–413, July 2000.
[5] T. I. Fossen and M. Blanke, "Nonlinear output feedback control of underwater vehicle propellers using feedback from estimated axial flow velocity," *IEEE J. Oceanic Eng.*, vol. 25, pp. 241–255, Apr. 2000.
[6] J. Farrell and B. Clauberg, "Issues in the implementation of an indirect adaptive control system," *IEEE J. Oceanic Eng.*, vol. 18, pp. 311–318, July 1993.
[7] J. Yuh, "Modeling and control of underwater robotic vehicles," *IEEE Trans. Syst., Man, Cybern.*, vol. 20, pp. 1475–1483, Nov. 1990.
[8] E. W. McGookin, "Reconfigurable sliding mode control for submarine manoeuvring," in *Proc. IEEE Oceans'01*, 2001, pp. 1775–1782.
[9] R. Cristi, F. A. Papoulias, and A. J. Healey, "Adaptive sliding mode control of autonomous underwater vehicles in the dive plane," *IEEE J. Oceanic Eng.*, vol. 15, pp. 152–160, July 1990.
[10] A. J. Healey and D. Lienard, "Multivariable sliding mode control for autonomous diving and steering of unmanned underwater vehicles," *IEEE J. Oceanic Eng.*, vol. 18, pp. 327–339, July 1993.
[11] P. M. Lee, S. W. Hong, Y. K. lim, C. M. Lee, B. H. Jeon, and J. W. Park, "Discrete-time quasi-sliding mode control of an autonomous underwater vehicle," *IEEE J. Oceanic Eng.*, vol. 24, pp. 388–395, July 1999.
[12] J. J. E. Slotine, J. K. Hedrick, and E. A. Misawa, "On sliding observers for nonlinear systems," *ASME J. Dyn., Meas., Control*, vol. 109, pp. 245–252, 1987.
[13] R. A. Masmoudi and J. K. Hedrick, "Estimation of vehicle shaft torque using nonlinear observers," *ASME J. Dyn., Meas., Control*, vol. 114, pp. 394–400, 1992.
[14] L. R. Ray, "Nonlinear tire force estimation and road friction identification: Simulation and experiments," *Automatica*, vol. 33, no. 10, pp. 1819–1833, 1997.
[15] M. Boutayeb, H. Rafaralahy, and M. Darouach, "Convergence analysis of the extended Kalman filter used as an observer for nonlinear deterministic discrete-time systems," *IEEE Trans. Automat. Contr.*, vol. 42, pp. 581–586, Apr. 1997.



**Joonyoung Kim** received the B.S. and M.S. degrees in naval architecture from Inha University, Incheon, Korea, in 1989 and 1993, respectively, and the Ph.D. degree in precision mechanical engineering from Hanyang University, Seoul, Korea, in 1991.

He is currently a Postdoctoral Fellow in the Department of Naval Architecture & Ocean Engineering, Seoul National University, Seoul, Korea. His research interests include monitoring and control for autonomous underwater vehicles.



**Kihun Kim** received the B.S. and M.S. degrees in naval architecture and ocean engineering from Seoul National University, Seoul, Korea, in 1998 and 2000, respectively. He is working toward the Ph.D. degree in the Department of Naval Architecture & Ocean Engineering at the same university, specializing in hydrodynamics, control, system identification, and estimation of hydrodynamic coefficient for autonomous underwater vehicles.



**Hang S. Choi** (M'00) received the B.S. and M.S. degrees in naval architecture from Seoul National University, Seoul, Korea, in 1970, and 1972, respectively, and the Ph.D. degree in civil engineering from the Technical University of Munich, Munich, Germany, in 1979.

He is currently a Professor in the Department of Naval Architecture & Ocean Engineering, Seoul National University. His research areas are marine hydrodynamics, motion and control of floating structures, and AUV design and control.



**Woojae Seong** was born in Seoul, Korea. He received the B.S. and M.S. degrees in naval architecture and ocean engineering from Seoul National University, Seoul, Korea, in 1982, and 1984, respectively, and the Ph.D. degree in ocean engineering from the Massachusetts Institute of Technology, Cambridge, in 1991.

He is currently an Associate Professor in the Department of Naval Architecture and Oceanic Engineering, Seoul National University. His current research interests are in acoustic propagation modeling in realistic ocean environments, geoacoustic inversions, and matched field processing.



**Kyu-Yeul Lee** received the B.S. degree in naval architecture from Seoul National University, Seoul, Korea, and the M.S. and Ph.D. degrees in naval architecture from the Technical University Hanover, Hanover, Germany, in 1975 and 1982, respectively.

He was Project Leader of the national project, "Computerized Ship Design and Production System." He is currently a Professor in the Department of Naval Architecture & Ocean Engineering, Seoul National University. His areas of specialty are optimization, geometric modeling, and CALS in shipbuilding.